Weld Morphology and Thermal Modeling in Dual-Beam Laser Welding

Weld morphology in dual-beam laser welding was investigated and mathematical modeling was performed to understand the impact of the heat flow pattern on dual-beam laser welds

BY J. XIE

ABSTRACT. Laser beam welding using two lasers, or dual-beam laser welding, is an emerging welding technology. An earlier experimental study (Ref. 1) showed use of the dual-beam laser welding technique could significantly improve weld quality for both steel and aluminum because process instability during laser welding was minimized. In the current study, weld morphology in dual-beam laser welding such as weld profiles, penetration depth, and weld width was experimentally investigated and the dual-beam laser process was mathematically modeled to understand the changes in heat flow pattern. It was found dual-beam laser welds had a wide width on the top surface of a workpiece, then narrowed down rapidly underneath the surface, forming a "nail" type weld. The penetration depth of dual-beam laser welds was less than single-beam laser welds in some conditions and a critical speed associated with the difference in penetration depth was identified based on experimental results. The penetration depth in dual-beam laser welding was less than that in single-beam laser welding at travel speeds below the critical speed and was the same at travel speeds above the critical speed. A laser melting experiment on an acrylic block indicated the keyhole in dual-beam laser welding was elongated, so there was a heat conduction loss along the longitudinal sides of the elongated keyhole leading to a reduction of penetration depth. An expression for the critical speed was obtained by comparing a travel speed to an expansion rate of a thermal layer in the transverse direction of the longitudinal sides. The predicted critical speed was 4.29 m/min for steel and 21.45 m/min for aluminum, respectively. A mathematical expression to predict the difference in penetration depth between single- and dual-beam

laser welding was developed and the theoretical values of the penetration difference agreed well with the experimental data. Further analysis showed penetration capability of dual-beam lasers decreased with the increase in interbeam spacing.

Introduction

Laser welding has been widely used in the automotive, aerospace, electronic, and medical industries to join a variety of materials because it offers a number of advantages over conventional joining processes such as low heat input, minimal distortion, high welding speeds, noncontact and precision processing, and good repeatability. However, a number of weld defects are often encountered in laser welds such as porosity, undercuts, spatter, humping, cracking, and surface holes. How to make high-quality and consistent laser welds is one of the major concerns of industry. A laser welding technique called dual-beam laser welding was investigated in an earlier study (Ref. 1) to quantify the benefits of dual-beam laser processing when a high-power CO_2 laser beam was split into two equal-power beams by a wedge mirror. The "split" or dual laser beams were almost parallel and interbeam spacing was as small as 1.2 mm from center to center. The dual laser beams moved in tandem during welding, as shown in Fig. 1. Experimental results showed use of the dual-beam laser could significantly improve weld quality for both steel and aluminum (Ref. 1). An investigation of the plasma plume above a workpiece in laser welding indicated the plasma plume in conventional single-beam laser welding was unstable and fluctuated at an average frequency of 1.2 kHz (Ref. 1). Plasma fluctuation is generally considered to be associated with the keyhole instability that results in poor welds. In the case of dual-beam laser welding, plasma fluctuation was suppressed by the dual-beam laser due to the elongated keyhole that contributed to improved keyhole stability. As a result, the stabilized process could lead to improved weld quality.

According to the earlier experimental study (Ref. 1), the split or dual laser beams were close enough to create a common keyhole. The effect of reducing keyhole instability no longer existed if the interbeam space was too large to generate one common keyhole. In the case of a large space (for example, 10 mm), two keyholes would be created and the cooling rate during laser welding might be reduced (Refs. 2, 3) instead of the effect of improving process stability with a small interbeam space.

In the earlier experiment, the small interbeam space created a common keyhole, as with conventional single laser beam welding. However, keyhole shape and heat flow pattern during dual-beam laser welding were totally different from that of single-beam laser welding. The changes that occurred in dual-beam laser welding would lead to the change in weld profile, weld size, penetration depth, cooling rate, and thermal stress around the weld pool. In the current study, weld morphology in dual-beam laser welding was compared to conventional single-beam laser welding and mathematical modeling was performed based on the heat conduction theory to understand dual-beam laser processing and its impact on laser welds.

KEYWORDS

Laser Welding
Dual Beam
Weld Quality
Mathematical Modeling
Heat Flow
Weld Profile
Penetration Depth
Weld Width
Elongated Keyhole
Critical Speed
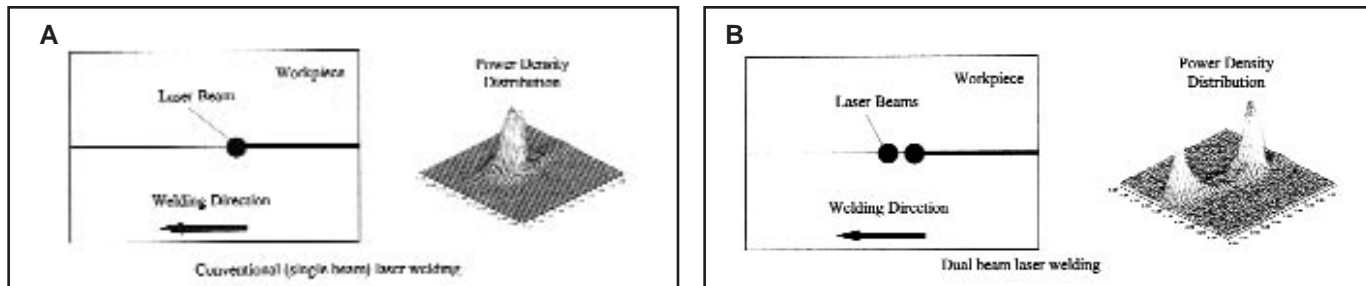Interbeam Spacing
Steel
Aluminum

Fig. 1 — Laser beam welding setups. A — Conventional (single-beam) laser welding; B — dual-beam laser welding.
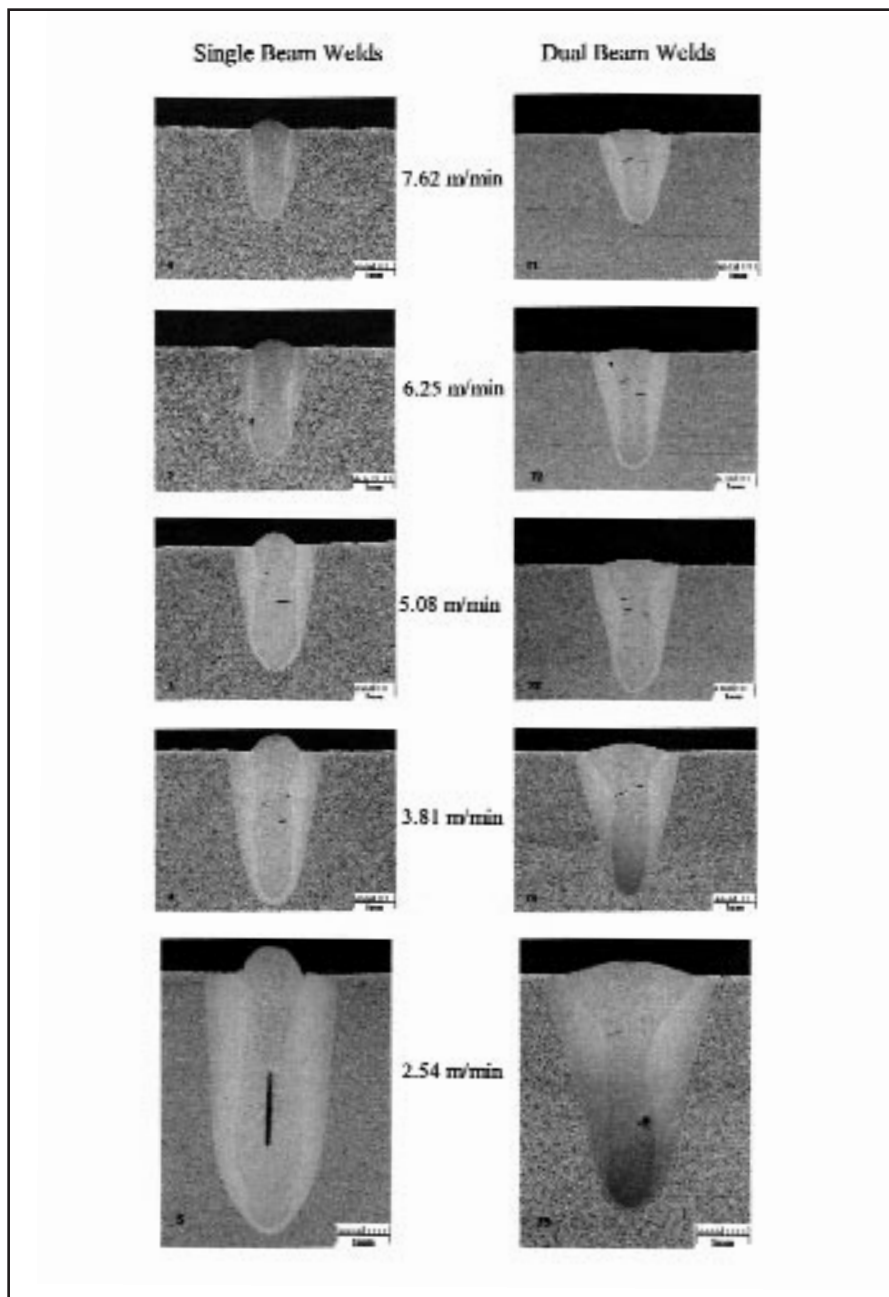

Fig. 2 — Steel weld profiles at various travel speeds (1045 steel, bead on plate, CO_2 laser, 6 kW). Single-beam welds are shown on the left and dual-beam welds on the right.

Experimental Studies

Both conventional single-beam and dual-beam laser welding were carried out using a 6-kW CO_2 laser. In dual-beam laser welding, the laser beam was split into two equal-power beams at an interbeam space of 1.2 mm from center to center. The dual laser beams were focused down on the workpiece surface with a 200-mm parabolic focusing mirror at a spot size of 0.5 mm. The dual CO_2 laser beams were almost parallel and moved in tandem during welding. The single- and dual-beam laser welding setups are shown in Fig. 1. For this study, laser power was kept at 6 kW; travel speeds varied from 0.625 to 7.62 m/min. For the dual laser beam setup, each split beam had a laser power of 3 kW and the total power of the dual beams was 6 kW. It was found all laser welds were in the keyhole welding mode in the speed range investigated, and coupling efficiency for both single- and dual-beam laser welding should be as high as 90% because of multiple reflections in the keyholes (Ref. 4).

Plates of 6.35-mm-thick 1045 steel and 6.0-mm-thick 5052 aluminum were used for the bead-on-plate welding experiment. Helium was used as the shielding gas to protect the weld pool from oxidizing and it was delivered to the welding area by a side jet at a flow rate of 20 L/min. Laser welds were cross sectioned, polished, etched, and photographed for weld profiles, and weld width and penetration depth were then measured.

Weld Profiles

In conventional single-beam laser welding, the welds are typically deep and narrow and have a high aspect ratio. In dual-beam laser welding, the welds still have a high aspect ratio, but the weld profile is slightly different from single-beam laser welds due to the change in keyhole shape and heat flow pattern. Weld profiles of dual-beam laser welds are compared to single-beam laser welds in Fig. 2. Since the 1045 steel used in the experiment had a medium carbon content (0.45% C), it was a crack-sensitive material for fusion weld-
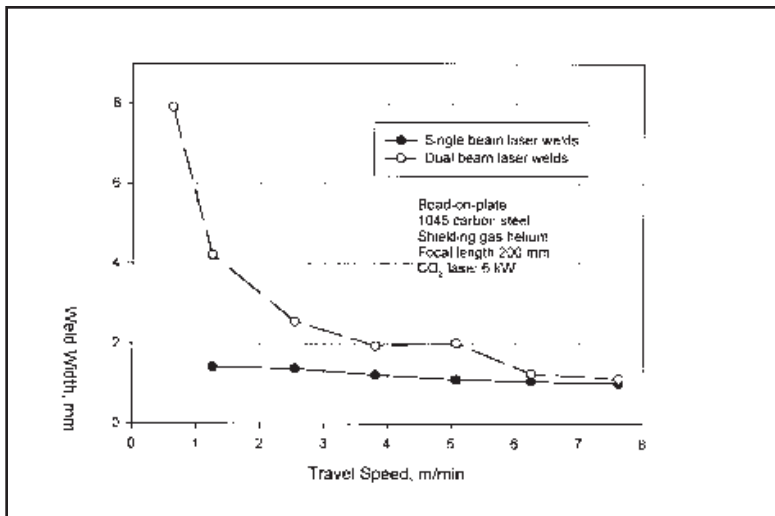
Fig. 3 — Steel weld width on the top surface.

Fig. 4 — Aluminum weld profiles (5052 aluminum alloy, bead on plate, CO_2 laser, 6 kW, 3.81 m/min). A — Single-beam laser weld; B — dual-beam laser weld.

ing. As a result, microcracks were found in some of the laser welds. Crack issues in single- and dual-beam laser welding were addressed in Ref. 1, so weld profile only is emphasized in this paper.

For single-beam welds, the weld width is almost identical along the direction of penetration depth. However, dual-beam laser welds have a wide width on the top surface and then narrow down like a nail, as shown in Fig. 2. The "nail" in the dual-beam laser welds can be seen obviously at low travel speeds. For example, at 2.54 m/min, which is considered a relatively low speed, the width of the single-beam laser weld does not vary greatly along the penetration depth, but the width of the dual-beam laser weld is much wider on the top surface, then is rapidly reduced to "normal size" along the penetration depth — Fig. 2. As a result, the difference in weld width between the single- and dual-beam laser processes is small at high travel speeds but changes significantly at low speeds, as shown in Fig. 3.

The 5052 aluminum welds were cross-sectioned for weld profiles in Fig. 4 and the weld width on the top surface was measured in Fig. 5. As expected, the width of the dual-beam laser weld is large on the top surface, but penetration depth is dramatically reduced when compared to the single-beam laser welds of aluminum. It can be seen from Fig. 5 that the width of the dual-beam laser welds is always greater than that of single-beam laser welds no matter what the travel speed is. The impact of dual-beam laser welding on steel and aluminum will be discussed more later.

Penetration Depth

Penetration depth is one of the most important characteristics of laser welds.

Penetration depth for both single- and dual-beam steel welds was measured, as shown in Fig. 6. The penetration depth of the dual-beam welds was less than that of the single-beam laser welds at low travel speeds but was almost the same at high travel speeds. When travel speed was lower than 4.3 m/min, the difference in penetration depth for single- and dual-beam laser welds increased with the increase in travel speeds.

A critical speed, v_{cr}, is defined as a speed boundary where the penetration depth in the dual-beam process is just less than that in single-beam laser welding — Fig. 6. Consequently, it could be said the penetration depth for both processes is different at travel speeds lower than the critical speed and is the same at speeds higher than the critical speed. The critical speed was found to be 4.3 m/min for steel according to the experimental data obtained in this investigation — Fig. 6. This difference in penetration depth at low travel speeds for both processes might be caused by changes in the keyhole shape that lead to a different heat flow pattern during welding. To understand the keyhole shapes in dual-beam laser processing, an acrylic block was irradiated by stationary single and dual laser beams for 100 ms at 3 kW. The top view of the plastic block after laser irradiation is shown in Fig. 7. As expected, the keyhole produced by the stationary single-beam laser is round, but the keyhole irradiated by the stationary dual-beam laser is elongated in the longitudinal direction due to the interbeam spaces.

Heat conduction flow patterns around the circular and elongated keyholes are depicted in Fig. 8. Obviously, in the case of the dual-beam laser process, extra heat is conducted away along the longitudinal sides 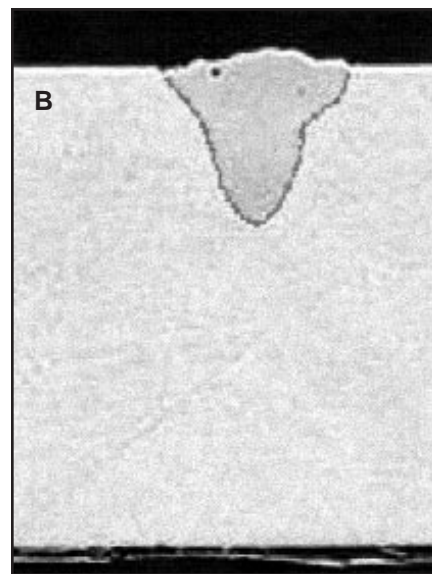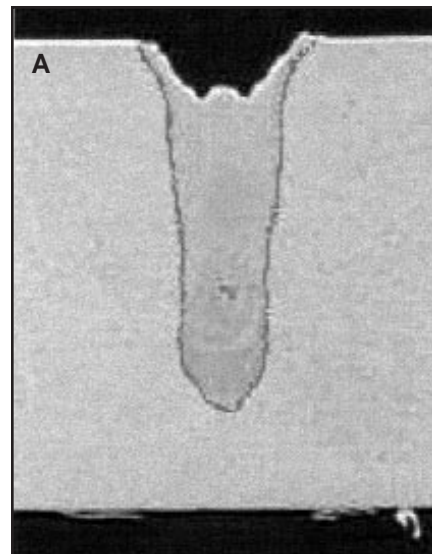of the elongated keyhole when com-pared to single-beam laser welding. The length of the longitudinal sides of the elongated keyhole is approximately equal to the interbeam spaces. The extra heat conduction loss could be the major reason causing the change in weld profiles and penetration depth in dual-beam laser welding.

When travel speed is in the range less than the critical speed, the extra heat conduction loss increases with the decrease in travel speed because laser/material interaction time is increased and more heat is conducted away along the longitudinal sides. The heat loss creates a temperature profile and a "thermal layer" in the Y axis, as shown in Fig. 8B. The thermal layer is defined as a distance beyond which there is no heat flow; hence, the initial temperature distribution remains unaffected be-
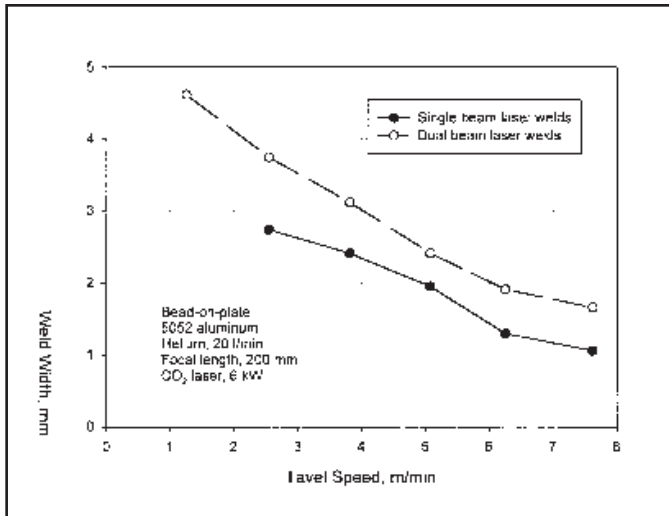
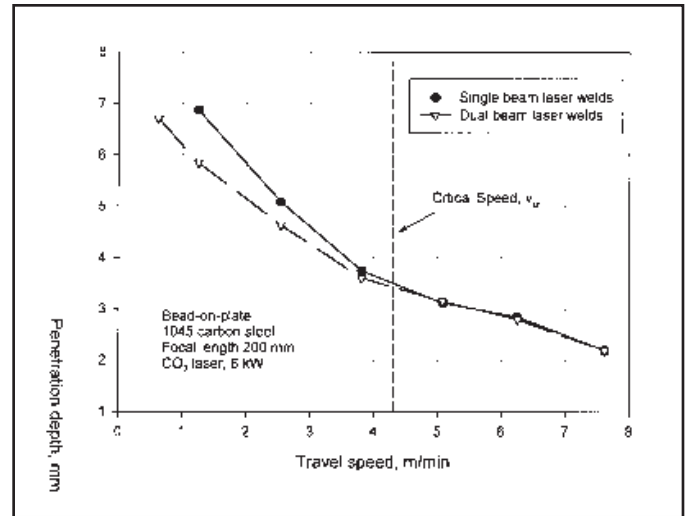*Fig. 5 — Aluminum weld width on the top surface.*
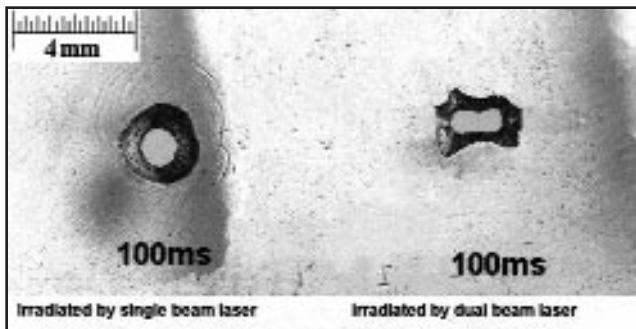

Fig. 6 — Penetration depth of steel welds.

Fig. 7 — Top view of an acrylic plastic after laser irradiation (3-kW, CO_2 laser, irradiation time 100 ms).

yond the thermal layer (Ref. 5). The thermal layer in the Y axis increases with the decrease in travel speeds or increased laser/material interaction time. In other words, the thermal layer "grows" with the interaction time.

When the travel speed is higher than the critical speed, it is believed the keyhole is still elongated because of the spacing between two split beams and the extra heat loss in the Y axis still occurs. However, the effect of the extra heat loss might be neglected because the travel speed could be equal to or higher than the "growth rate" or "expansion rate" of the thermal layer in magnitude in the Y axis. In this case, the laser energy in dual-beam laser welding is utilized to create a keyhole as "efficiently" as in single-beam laser welding. As a result, the penetration depth of dual-beam laser welds is the same as that of single-beam laser welds at travel speeds higher than the critical speed.

Mathematical Modeling

To better understand the laser processes, mathematical modeling was performed to analyze the change in heat flow pattern in dual-beam laser welding and its influences on weld characteristics.

Critical Speed

According to the previous analysis of the dual-beam laser process, heat conduction loss along the longitudinal sides of the elongated keyhole creates a thermal layer; the effect of the extra heat loss could be neglected at the travel speed higher than the critical speed. In this case, the travel speed should be equal to or higher than the expansion rate of the thermal layer. The critical speed can, therefore, be estimated by comparing the expansion rate to travel speed in dual-beam laser welding.

According to the heat conduction theory (Ref. 5), thermal layer (δ) is approximated as

$$\delta = 4\sqrt{\alpha t} \qquad (1)$$

where α is the thermal diffusivity of material and t is the time of heat conducting. In dual-beam laser welding, the "thermal layer" in Equation 1 can be considered as the layer starting from the edge of the elongated keyhole in the transverse direction — Fig. 8B. The temperature at this keyhole edge is assumed to be the boiling point of the material, T_V. Then, the average expansion rate of the thermal layer in the transverse direction (Y axis), v_{TL}, is approximately derived from dividing

Equation 1 by time t

$$v_{TL} = \frac{\delta}{t} = \frac{4\sqrt{\alpha}}{\sqrt{t}} \qquad (2)$$

where time t should be considered as the laser/materials interaction time in laser welding. The interaction time in dual-beam laser welding can be estimated as the following:

$$t = \frac{L_0 + d_0}{v} \qquad (3)$$

where v is the travel speed, d_0 is the keyhole width of the elongated keyhole that is roughly the same as the keyhole diameter in single-beam laser welding, and L_0 is the length of the elongated keyhole from center to center that is approximately equal to the interbeam spacing as shown in Fig. 8B. According to the definition of the critical speed and analysis of heat conduction loss, the travel speed should be equal to the expansion rate of the thermal layer (v_{TL}) at the critical speed where the extra heat loss could be neglected. Therefore, the critical travel speed is obtained by substituting Equation 3 into Equation 2:

$$v_{cr} = \frac{16\alpha}{L_0 + d_0} \qquad (4)$$

where the thermal diffusivity (α) of materials in the liquid state should be used in Equation 4 because the elongated keyhole is surrounded by molten metal and the extra heat loss is conducted away from the keyhole edge into molten metal in the weld pool. According to the expression in Equation 4, the critical speed is dependent on the dimensions of the elongated keyhole and physical properties of the material. Generally, the dimensions of the elon-
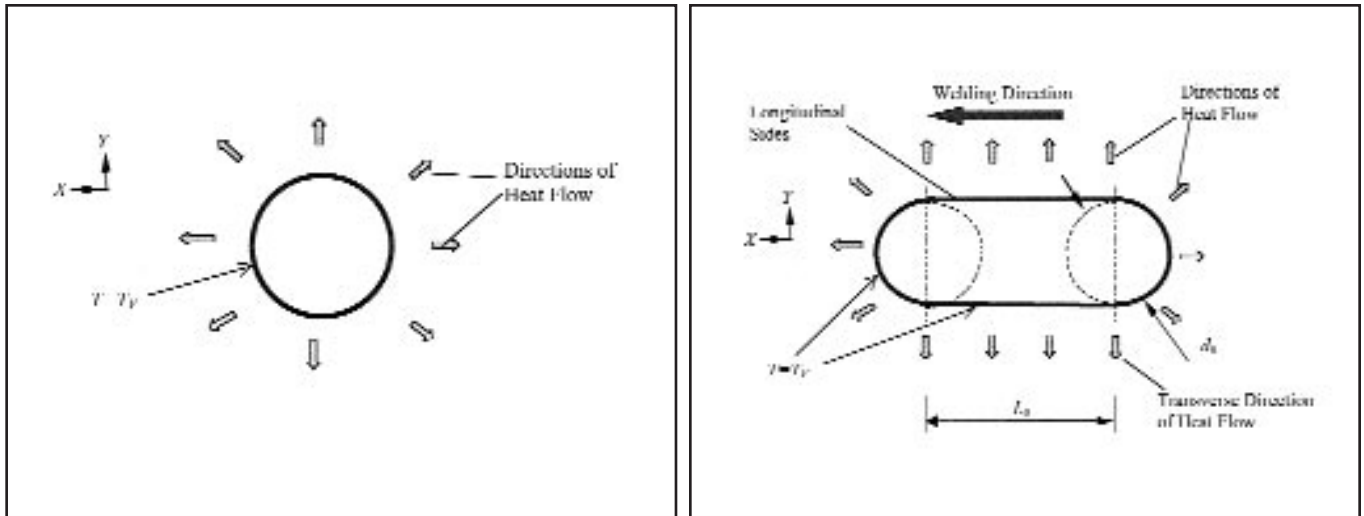
Fig. 8 — Heat conduction flows around keyholes in laser welding. A — Heat flow around the circular keyhole in single-beam laser welding; B — heat flow around the elongated keyhole in dual-beam laser welding.

gated keyhole can be varied only in a small range to have one common keyhole (Ref. 1), so the material property would be the major variable affecting the critical speed. The critical speeds for some metals were calculated in Table 1 based on the dual-beam CO_2 laser setup with an interbeam space of 1.2 mm and assumed keyhole diameter of 0.5 mm. The critical speed was found to be 4.29 m/min for steel, which was in good agreement with the experimental result as shown in Fig. 6.

For aluminum, the calculated critical speed is as high as 21.5 m/min because of aluminum's high thermal diffusivity (Table 1). As a result, a lot of laser energy is conducted away along the longitudinal sides of the elongated keyhole during dual-beam laser welding of aluminum. The predicted critical speed of aluminum is much higher than the travel speeds often used in industry, so the penetration depth in the dual-beam laser process is expected to be less than in single-beam laser welding in the "common" range of travel speeds. The penetration depth of 5052 aluminum welds was measured for both processes in Fig. 9. The penetration depth of the dual-beam laser welds is always less than that of single-beam laser welds, but the difference in penetration depth decreases as travel speed increases and it tends to approach the predicted critical speed of 21.5 m/min.

In complete-penetration butt-joint welding, a higher laser power is needed to compensate for the extra heat conduction loss in dual-beam laser welding, especially for aluminum welding. For example, to obtain complete-penetration butt-joint welds of 3-mm 5083 aluminum plates, a laser power of 4.5 kW was needed in dual-beam laser welding while 3.0 kW was good enough in conventional single-beam laser

welding at a travel speed of 3.81 m/min.

In general, a simple expression for the critical speed was derived from the thermal layer surrounding the elongated keyhole. To have an exact expression for the critical speed, a three-dimensional temperature profile induced by the dual-beam laser should be obtained and then the extra heat loss and expansion rate of the thermal layer in the Y axis could be calculated. However, the procedures would be complicated because the exact temperature profile and the expansion rate of the thermal layer are difficult to compute. In this study, the concept of "thermal layer" was introduced and some assumptions were made to calculate the expansion rate of the thermal layer such as one-dimensional heat conduction, linear temperature distribution, and neglecting solid/liquid phase change. As a result, Equation 4 is an approximate estimation for the critical speed but it is simple and easy to use. The simple expression was also found to be in good agreement with the available experimental data.

Penetration Depth

As mentioned earlier, penetration depth of dual-beam laser welds was less than single-beam laser welds at the travel

speed of less than the critical speed. To further understand the change in penetration depth in the dual-beam laser process, a mathematical model to predict the penetration depth was developed by using a single-beam laser welding model developed by Lankalapalli et al. (Ref. 6). In this two-dimensional model for single-beam laser welding, the keyhole was assumed to be conical in the depth direction because the majority of normal laser welds tapered down (Ref. 6). The governing equation and boundary conditions for the temperature distribution in single-beam laser welding were described by Carslaw and Jaeger (Ref. 7)

$$\frac{\partial^2 T(x,y)}{\partial x^2} + \frac{\partial^2 T(x,y)}{\partial y}$$
$$= -\frac{v}{\alpha}\frac{\partial T(x,y)}{\partial x} \qquad (5)$$

$$T(x,y) = T_v \quad at \quad x^2 + y^2 = d_0^2 \quad (6)$$

$$T(x,y) \rightarrow T_0 \quad as \quad x,y \rightarrow \pm\infty \quad (7)$$

where $T(x,y)$ is the temperature distribution around the keyhole, T_V is the vaporization temperature of the material, T_0 is

Table 1 — Critical Speeds for Some Metals[a]

	Iron	Aluminum	Stainless Steel	Copper	Titanium
Thermal Diffusivity, $(\times 10^6 \text{ m}^2/\text{s})$	7.6	38	4.9	43	8.2
Critical Speed, (m/min)	4.29	21.45	2.77	24.28	4.65

(a) Assuming $L_0 = 1.2$ mm and $d_0 = 0.5$ mm in Equation 4.
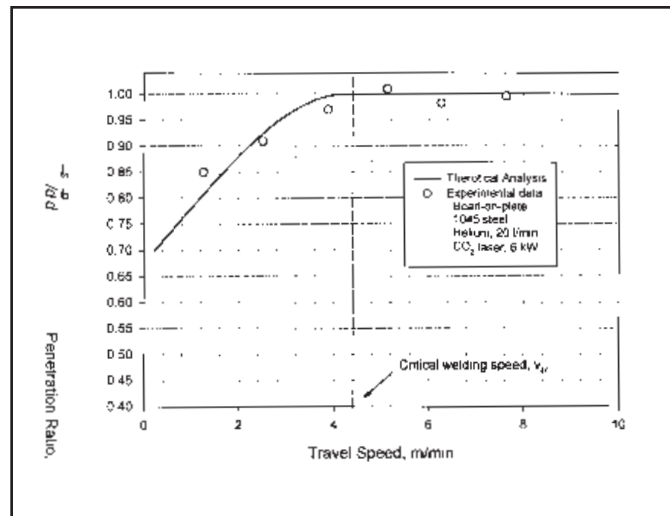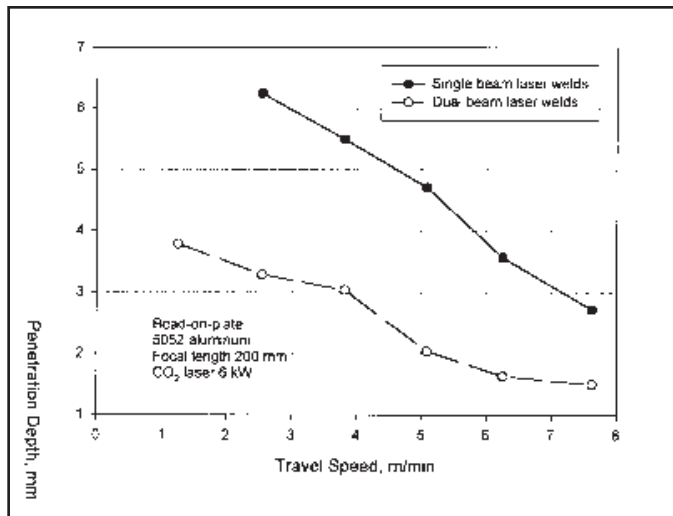
Fig. 9 — Penetration depth of aluminum welds.

Fig. 10 — Penetration ratio of steel welds.

the initial temperature, d_0 is the keyhole diameter on the surface, and x and y are axes in Cartesian coordinate. Lankalapalli et al. (Ref. 6) calculated the average temperature gradient around the keyhole based on Carslaw and Jaeger's solution to Equations 5–7, which is

$$\left(\frac{\partial T}{\partial r*}\right)_{ave} = -\left(T_V - T_0\right)G\left(P_e\right) \quad (8)$$

where

$$G(P_e) = C_1 + C_2 P_e + C_3 P_e^2 + C_4 P_e^3 \quad (9)$$

Here, $r*$ is the normalized radius of the keyhole, P_e is the Peclet number at a penetration depth of $z(P_e = vd/2\alpha)$, d is the keyhole diameter at penetration z, and the coefficients $C_1 = 2.1995$, $C_2 = 6.962$, $C_3 = -0.4994$, and $C_4 = 0.0461$. The penetration depth in single-beam laser welding was obtained by integrating the laser power absorbed along the penetration depth (Ref. 6)

$$\bar{d}_s = \frac{P}{k\left(T_V - T_0\right)} \frac{1}{\sum_{i=1}^{4} \frac{C_i}{i}\left(P_{e0}\right)^{i-1}} \quad (10)$$

where d_s is the penetration depth in single-beam laser welding, P is the incident laser power, k is the thermal conductivity of the material, and P_{e0} is the Peclet number on the top surface $(P_{e0} = vd_0/2\alpha)$. This expression for penetration depth was said to be in good agreement with the experimental data on single-beam laser welding of steel (Ref. 6).

In dual-beam laser welding, there is an extra heat conduction loss along the longitudinal sides of the elongated keyhole, as described in Fig. 8. To predict penetration depth in the dual-beam laser process, it is necessary to know the amount of the extra heat conduction loss in the transverse direction. According to the Fourier law, the extra heat loss per unit depth on both longitudinal sides of the elongated keyhole is

$$P_{loss} = -2k\left(\frac{\partial T}{\partial y}\right)\Big|_{y=d_0/2} \quad (11A)$$

and the temperature gradient in Equation 11A can be estimated from Equation 8 by considering the entire side length of the elongated keyhole, yielding the following:

$$\left(\frac{\partial T}{\partial y}\right)\Big|_{y=d_0/2} = -\left(T_V - T_0\right)G\left(P_e\right)\left(\frac{L_0}{\pi d_0}\right) \quad (11B)$$

When travel speed is greater than critical speed, the extra heat loss in Equation 11 is very little and could be neglected. Therefore, a nondimensional term related to the critical speed, $(1-v)/v_{cr}$, should be considered in expression of the extra heat loss. Since the heat conduction loss is not linearly proportional to interaction time, a quadratic relation of the nondimensional term is intentionally put in Equation 11B, so Equation 11A becomes:

$$P_{loss} = 2k\left(T_V - T_0\right)G\left(P_e\right) \left[\frac{L_0}{\pi d_0}\left(1 - \frac{v}{v_{cr}}\right)\right]^2 \quad (12)$$

The absorbed power per unit depth (P_t) in dual-beam laser welding then becomes

$$P_t = P_z + P_{loss} = k\left(T_V - T_0\right)G\left(P_e\right) \left\{1 + 2\left[\frac{L_0}{\pi d_0}\left(1 - \frac{v}{v_{cr}}\right)\right]^2\right\} \quad (13)$$

where P_z is the laser power absorbed per unit depth in single-beam laser welding (Ref. 6). The total absorbed laser power determined by integrating Equation 13 along the entire penetration depth is equal to the incident laser power:

$$P = \int_0^{\bar{d}_D} P_t\left(z\right)dz \quad (14)$$

Where $\bar{d}_D$ is the penetration depth in dual beam laser welding. The Peclet number, P_e, is a function of z according to the assumption of the conical keyhole in the depth direction, and then the boundary conditions on the top and bottom surfaces are given as

$$P_e\left(0\right) = \frac{vd_0}{2\alpha} \qquad at\ z = 0 \quad (15)$$

and then

$$P_e\left(\bar{d}_D\right) = 0 \qquad at\ z = \bar{d}_D \quad (16)$$

The relationships between the Peclet number and penetration depth can then be estimated as (Ref. 6)
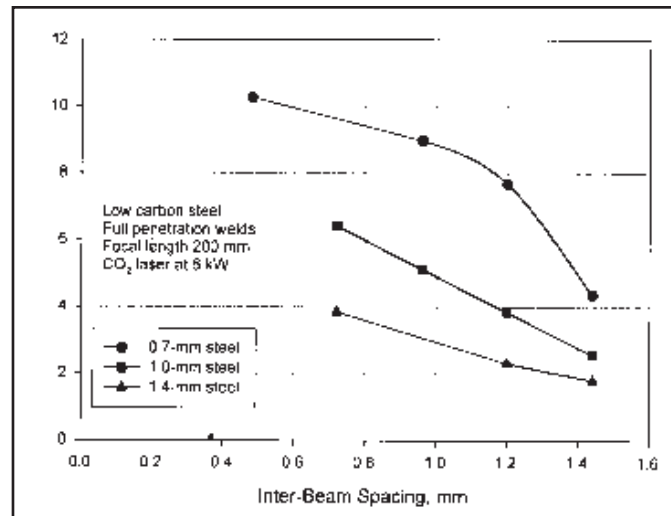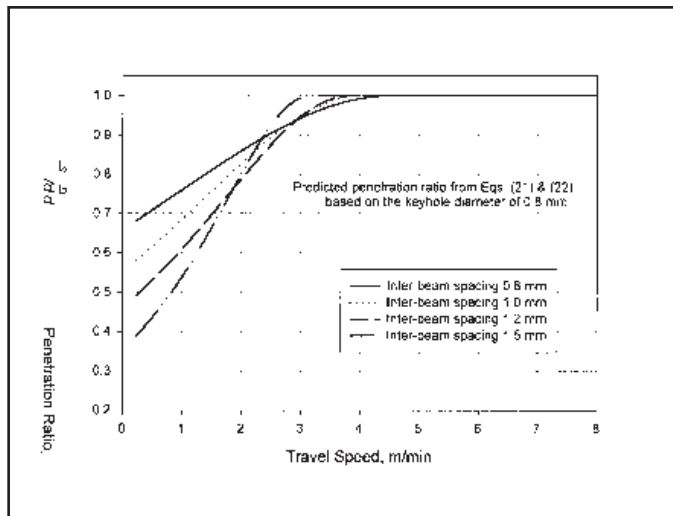
Fig. 11 — Predicted penetration ratio of steel welds at various interbeam spaces.

Fig. 12 — Maximum welding speed at various interbeam spaces.

$$P_e(z) = P_{e0}\left(1 - \frac{z}{\bar{d}_D}\right) \qquad (17)$$

and

$$dz = -\frac{\bar{d}_D}{P_{e0}} dP_e \qquad (18)$$

Substituting Equations 13, 17, and 18 into Equation 14, we obtain

$$P = \frac{\bar{d}_D k \left(T_V - T_0\right)}{P_{e0}}$$

$$\left\{1 + 2\left[\frac{L_0}{\pi d_0}\left(1 - \frac{v}{v_{cr}}\right)\right]^2\right\}$$

$$\int_0^{P_{e0}} G\left(P_e\right) dP_e \qquad (19)$$

where $G(P_e)$ is given in Equation 9. Thereby, the expression for the penetration depth in dual-beam laser welding, $\bar{d}_D$, is solved as

$$\bar{d}_D =$$

$$\frac{P}{k\left(T_V - T_0\right)\left\{1 + 2\left[\frac{L_0}{\pi d_0}\left(1 - \frac{v}{v_{cr}}\right)\right]^2\right\}\sum_{i+1}^4 \frac{C_i}{i}\left(P_{e0}\right)^{i-1}}$$

$$when \; v \le v_{cr} \qquad (20)$$

The ratio of the penetration depth in the single- and dual-beam laser processes is derived from Equations 10 and 20:

$$\frac{\bar{d}_D}{\bar{d}_S} = \frac{1}{1 + 2\left[\frac{L_0}{\pi d_0}\left(1 - \frac{v}{v_{cr}}\right)\right]^2}$$

$$when \; v \le v_{cr} \qquad (21)$$

When the travel speeds are greater than the critical speed, the ratio is

$$\frac{\bar{d}_D}{\bar{d}_S} = 1 \quad when \; v \ge v_{cr} \qquad (22)$$

From Equation 21, it can be seen that the difference in penetration depth or penetration ratio, $(\bar{d}_D/\bar{d}_S)$, is a function of the dimensions of the elongated keyhole and travel speed. The dimensions of the elongated keyhole could be approximately estimated by the characteristics of the dual laser beams; determining the exact dimensions of the elongated keyhole is difficult. As a result, the length of the elongated keyhole (L_0) is approximately equal to the interbeam spacing and the keyhole diameter is slightly bigger than the laser beam diameters. In this study, the penetration ratio was estimated by using an interbeam space of 1.2 mm and an assumed keyhole diameter of 0.8 mm. The theoretical results were then compared with the experimental data in Fig. 10. It was found the predicted values of the penetration ratio were in good agreement with the experimental data.

As discussed in the earlier study (Ref. 1), interbeam spacing is an important variable in dual-beam laser welding. The penetration ratio $(\bar{d}_D/\bar{d}_S)$ at various interbeam spaces was plotted against travel speeds in Fig. 11 according to the mathematical expression for the penetration ratio in Equations 21 and 22. It shows the penetration ratio decreases significantly with the increase in interbeam spaces at low travel speeds. Such a change in penetration ratio is associated with heat conduction loss along the longitudinal sides of the elongated keyhole. As interbeam space increases, the heat conduction loss is accordingly increased and the penetration depth is further reduced. In other words, penetration depth in dual-beam laser welding is expected to be further reduced when the interbeam space increases. This conclusion has been experimentally verified in complete-joint-penetration welding of steel sheets.

In the complete-joint-penetration welding experiment, various interbeam spaces were used to weld 0.7-, 1.0-, and 1.4-mm steel sheets in a lap joint configuration. A maximum welding speed, which is defined as the maximum travel speed at which the laser beam just penetrates through the total thickness, was compared in various welding conditions. It was found the maximum welding speed decreased with the increase in interbeam space, as shown in Fig. 12. This means the dual-beam laser becomes too "weak" to penetrate through a workpiece as the interbeam space increases due to the increased heat conduction loss along the longitudinal sides of the elongated keyhole.

As mentioned in an earlier study (Ref. 1), the effect of improving weld quality using dual-beam lasers was based on the assumption a small interbeam space created one common keyhole. When the interbeam space is increased to be higher than a limit, the welding mode could be

changed to two keyholes in one weld pool or two keyholes in two separate weld pools. In this case, the mechanism of dual-beam laser welding could be completely different and the equations and conclusions obtained in this study are no longer valid.

Conclusions

1) The profile of dual-beam laser welds was slightly different from that of conventional single-beam laser welds. The dual-beam laser welds were wide on the top surface of a workpiece, then narrowed down rapidly like a "nail."

2) The keyhole was elongated in dual-beam laser welding due to the existence of the interbeam spaces. As a result, there was an extra heat conduction loss along the longitudinal sides of the elongated keyhole during welding when compared to single-beam laser welding. The penetration depth in dual-beam laser welding was found to be less than that in conventional single laser beam welding in some cases because of the extra heat conduction loss.

3) There was a critical speed associated with the difference in the weld morphology and penetration depth between single- and dual-beam laser welding. The

weld morphological difference was pronounced at travel speeds less than the critical speed and was small at speeds higher than the critical speed. The penetration depth of dual-beam laser welds was smaller than in single-beam laser welds when travel speed was lower than the critical speed, but was the same at travel speeds above the critical speed.

4) A mathematical expression for the critical speed was obtained by analyzing the heat conduction loss along the longitudinal sides of the elongated keyhole. The critical speed was a function of dimensions of the elongated keyhole and material properties. The predicted critical speed was found to be 4.29 m/min for steel; it was extremely high for aluminum (21.5 m/min). Therefore, the penetration depth of dual-beam laser welds for aluminum is always less than single-beam laser welds at the welding speeds usually used in industry.

A mathematical model was developed to predict penetration depth of dual-beam laser welds and the ratio of penetration depth between single- and dual-beam laser welding. The predicted penetration ratio was favorable to the experimental results of steel.

6) The increase in interbeam space

would result in the further decrease in penetration depth in dual-beam laser welding due to the increased heat conduction loss along the longitudinal sides of the elongated keyhole. In other words, the penetration capability of dual-beam lasers was reduced when the interbeam space increased.

References

1. Xie, J. 2001. Dual-beam laser welding. *Welding Journal* 81(9): 223-s to 230-s.

2. Liu, Y. N., and Kannatey-Asibu, E., Jr. 1997. Experimental study of dual-beam laser welding of AISI 4140 steel. *Welding Journal* 76(9): 342-s to 348-s.

3. Liu, Y. N., and Kannatey-Asibu, E., Jr. 1992. Laser Beam Welding with Simultaneous Gaussian Laser Preheating, Precision Machining: Technology and Machine Development and Improvement, Winter Annual Meeting of the ASME, Anaheim, Calif., pp. 191–202.

4. Steen, W. 1991. *Laser Materials Processing*, New York, N.Y.: Springer-Verlag.

5. Ozisik, M. N. 1993. *Heat Conduction*, 2nd ed. John Wiley & Sons, pp. 335–339.

6. Lankalapalli, K. N., Tu, J. F., and Gartner, M. 1996. A model for estimating penetration depth of laser welding processes. *Journal of Physics D: Applied Physics* 29: 1831–1841.

7. Carslaw, H. S., and Jaeger, J. C. 1962. *Conduction of Heat in Solids*, 2nd ed. New York, N.Y.: Oxford University Press p. 390.